THERMOVISCOUS DISSIPATION ON WAVE PROPAGATION IN CONICAL-CONFINED PIPELINE

Zheng Li[1], Yong Chen[1], Chengguang Fan[1], Yang Shi[1], Xiaohua Gan[1], Bo Yuan[2]

[1]College of Aerospace Science and Engineering, National University of Defense Technology, 410073, Changsha, China
email: literature.chen@gmail.com.

[2]Department of Machinery and Electrical Engineering, Logistical Engineering University, Chongqing, 401311, China
email: ramboyuanbo@aliyun.com.

Wave propagation in conical pipeline is of great interest in connection with ultrasonic flow measurement and horn acoustics. Theoretical researches for sound propagation in the conical duct concentrate on the isentropic wave propagation for the cases of stationary fluid and moving fluid. Moreover, excellent work on electromagnetic field theory of conical horns has been done by literature research. However, research on the wave propagation in cones considering the effect of thermoviscous dissipation is not complete as of today to the present authors' knowledge. This paper concentrates on the influence of thermoviscous dissipation on the axisymmetric wave propagation in a conical duct. Based on the conservations of mass, momentum and energy, mathematical deduction of linear viscothermal flow acoustics is presented. Moreover, solution based on complex function theory is given to solve the wavenumber. Numerical calculation concentrates on the analysis of phase velocity and attenuation of acoustic modes.

Keywords: thermoviscous dissipation, conical-confined pipeline, viscothermal wave propagation.

1. Introduction

Wave propagation in a pipeline flow is of great interest in both theoretical researches and industrial applications[1-5]. In the aircraft engineering, for example, particular considerations are placed on the prediction and suppression of engine noises[6-9]. The prediction of aero-acoustic features is also important in the catalytic converter design of a transport system[10, 11]. In the ultrasonic pipeline flow measurement[12-14], accurate prediction of ultrasonic wave propagation is of great importance on the improvement of measurement performance.

While researches on viscothermal wave propagation in cylindrical or rectangular pipelines have been comprehensively reported in the literature [15-19], research on wave propagation in the conical pipeline is not enough. In the case of plane wave propagation, Davies and Doak [20, 21] gave primary discussion under the effect of a mean flow in a conical pipeline. Easwaran and Munjal [22] deduced the transfer matrices of one-dimensional wave propagation at flow Mach number for conical and exponential pipeline shapes. In the book of Munjal [23], the author gave detailed deduction of plane wave in a conical duct. Comprehensive review of one-dimensional wave propagation can found in Mimani [24] and Willatzen [25]

Multi-dimensional wave propagation in conical pipelines has also received considerable interest. Astley and Eversman addressed multi-modal wave propagation in non-uniform ducts with mean flow using the weighted residual method[26] and FEA[27]. Willatzen [25] mathematically deduced axisymmetric 3-D wave propagation in a rigid-wall condical duct carrying a mean flow by means of an analytical Green's function based on the modal expansion of the acoustic field expressed in terms of Legendre functions of non-integer degree and the spherical Hankel functions. Mimani [24] extended to consider the azimuthal modes.

The aforementioned papers either analyse acoustic wave propagation in a variable area duct based on the simple 1-D plane/spherical wave model or whilst considering multi-dimensional wave propagation. However, the problem of analysing the acoustic attenuation behaviour due to the thermoviscous dissipation is not investigated yet. The objective of this paper is therefore, to analyse the effect of thermoviscous dissipation on the axisymmetric 3-D wave propagation in a conical pipeline.

This paper is organised as follows. Section 2 presents the theoretical formulation for axisymmetric 3-D viscothermal wave propagation confined by a conical duct using a semi-analytical approach based on the complete modal expansion. Section 3 presents the corresponding isentropic model in the case of an inviscid fluid. Section 4 gives some numerical discussions about the local wave number while section 5 gives the conclusion.

2. Mathematical formulation

Consider a truncated conical waveguide of radii a and b ($a<b$) and opening angle θ_0 as shown in Figure 1. Assume that the fluid is stationary and a linear disturbance is present and propagates along the conical pipeline. Spherical coordinates are chosen to represent the cone in the sense that the product of intervals

$$I_r \times I_\theta \times I_\Phi = [a;b]\times[0;\theta_0]\times[0;2\pi], \tag{1}$$

spans the whole truncated cone. As present paper concentrates on axisymmetric wave with respect to the Φ coordinates, acoustic waves are assumed to be dependent on the r and θ coordinates.

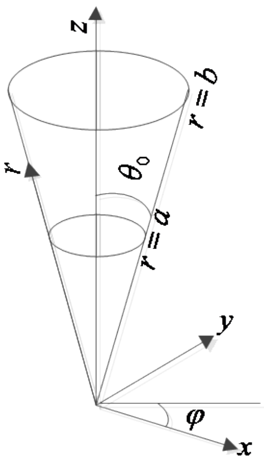

Fig. 1. Schematic diagram of a conical-confined pipeline

Under the stationary flow, the conservation of mass, momentum, and energy can be expressed as

$$\frac{\partial \rho'}{\partial t}+\rho_0\nabla\cdot\mathbf{v}'=0, \rho_0\frac{\partial \mathbf{v}'}{\partial t}=-\nabla p'+\eta\nabla^2\mathbf{v}'+\frac{\eta}{3}\nabla\left(\nabla\cdot\mathbf{v}'\right), \rho_0 T_0\frac{\partial s'}{\partial t}=\kappa_{\text{th}}\nabla^2 T'. \tag{2}$$

As the monofrequency operation is preferred, $\partial/\partial t$ can be replaced by $\mathrm{i}\omega$, thus one have

$$\mathrm{i}\omega\rho'+\rho_0\nabla\cdot\mathbf{v}'=0, \mathrm{i}\omega\rho_0\mathbf{v}'=-\nabla p'+\eta\nabla^2\mathbf{v}'+\frac{\eta}{3}\nabla\left(\nabla\cdot\mathbf{v}'\right), \mathrm{i}\omega\rho_0 T_0 s'=\kappa_{\text{th}}\nabla^2 T'. \tag{3}$$

According to the acoustic equations, one obtains that $s'=\left(c_p/T_0\right)T'-\left(1/\left(\rho_0 T_0\right)\right)p'$, then one obtains

$$\mathrm{i}\omega\rho_0 c_p T'-\mathrm{i}\omega p'=\kappa_{\text{th}}\nabla^2 T' \tag{4}$$

According to the state equation of the perfect gas with $p=\rho R_0 T$, one obtains

$$p' = \rho_0 R_0 T' - \frac{\rho_0 R_0 T_0}{\mathrm{i}\omega} \nabla \cdot \mathbf{v}'. \tag{5}$$

Substituting Eq. (5) into the second equation of Eq. (3) and Eq. (4) yields

$$\mathrm{i}\omega \mathbf{v}' = -R_0 \nabla T' + \frac{R_0 T_0}{\mathrm{i}\omega} \nabla(\nabla \cdot \mathbf{v}') + \frac{\eta}{\rho_0} \nabla^2 \mathbf{v}' + \frac{\eta}{3\rho_0} \nabla(\nabla \cdot \mathbf{v}'), \nabla \cdot \mathbf{v}' = \frac{\kappa_{\mathrm{th}}}{\rho_0 R_0 T_0} \nabla^2 T' - \frac{\mathrm{i}\omega c_p}{\gamma R_0 T_0} T'. \tag{6}$$

Divergence of the first equation and substituting the second equation yield

$$\left(1 + \frac{\mathrm{i}4\omega\eta}{3\rho_0 R_0 T_0}\right) \frac{\kappa_{\mathrm{th}}}{\rho_0 c_p} \nabla^4 T' - \left(\mathrm{i}\omega - \frac{4\omega^2\eta}{3\gamma\rho_0 R_0 T_0} - \frac{\omega^2 \kappa_{\mathrm{th}}}{\rho_0 R_0 T_0 c_p}\right) \nabla^2 T' - \frac{\mathrm{i}\omega^3}{\gamma R_0 T_0} T' = 0. \tag{7}$$

It is convenient to factorize the Eq. (7) as

$$\left(\nabla^2 + \Psi_1\right)\left(\nabla^2 + \Psi_2\right) T' = 0, \tag{8}$$

where

$$\Psi_1 = \frac{\left(\mathrm{i}\omega - \frac{4\omega^2\eta}{3\gamma\rho_0 R_0 T_0} - \frac{\omega^2 \kappa_{\mathrm{th}}}{\rho_0 R_0 T_0 c_p}\right) + \sqrt{\left(\mathrm{i}\omega - \frac{4\omega^2\eta}{3\gamma\rho_0 R_0 T_0} - \frac{\omega^2 \kappa_{\mathrm{th}}}{\rho_0 R_0 T_0 c_p}\right)^2 + 4\frac{\mathrm{i}\omega^3}{\gamma R_0 T_0}\left(1 + \frac{\mathrm{i}4\omega\eta}{3\rho_0 R_0 T_0}\right)\frac{\kappa_{\mathrm{th}}}{\rho_0 c_p}}}{-2\left(1 + \frac{\mathrm{i}4\omega\eta}{3\rho_0 R_0 T_0}\right)\frac{\kappa_{\mathrm{th}}}{\rho_0 c_p}} \tag{9}$$

$$\Psi_2 = \frac{\left(\mathrm{i}\omega - \frac{4\omega^2\eta}{3\gamma\rho_0 R_0 T_0} - \frac{\omega^2 \kappa_{\mathrm{th}}}{\rho_0 R_0 T_0 c_p}\right) - \sqrt{\left(\mathrm{i}\omega - \frac{4\omega^2\eta}{3\gamma\rho_0 R_0 T_0} - \frac{\omega^2 \kappa_{\mathrm{th}}}{\rho_0 R_0 T_0 c_p}\right)^2 + 4\frac{\mathrm{i}\omega^3}{\gamma R_0 T_0}\left(1 + \frac{\mathrm{i}4\omega\eta}{3\rho_0 R_0 T_0}\right)\frac{\kappa_{\mathrm{th}}}{\rho_0 c_p}}}{-2\left(1 + \frac{\mathrm{i}4\omega\eta}{3\rho_0 R_0 T_0}\right)\frac{\kappa_{\mathrm{th}}}{\rho_0 c_p}} \tag{10}$$

Expanding Eq. (8) into spherical polar coordinates yields

$$\frac{1}{r^2 \sin\theta}\left[\sin\theta \frac{\partial}{\partial r}\left(r^2 \frac{\partial T'}{\partial r}\right) + \frac{\partial}{\partial\theta}\left(\sin\theta \frac{\partial T'}{\partial\theta}\right)\right] + \Psi_1 T' = 0, \tag{11}$$

$$\frac{1}{r^2 \sin\theta}\left[\sin\theta \frac{\partial}{\partial r}\left(r^2 \frac{\partial T'}{\partial r}\right) + \frac{\partial}{\partial\theta}\left(\sin\theta \frac{\partial T'}{\partial\theta}\right)\right] + \Psi_2 T' = 0, \tag{12}$$

under the assumption of azimuthal symmetrical wave excitations. By separating the acoustic disturbance in functions depending on $r \in [a,b]$ and $\theta \in [-\theta_0, \theta_0]$ only:

$$T' = f(r) g(\theta), \tag{13}$$

Eqs. (11)-(12) can be expanded into

$$\frac{1}{f(r)} \frac{\mathrm{d}}{\mathrm{d}r}\left(r^2 \frac{\mathrm{d}f(r)}{\mathrm{d}r}\right) + \Psi_1 r^2 = -\frac{1}{\sin\theta g(\theta)} \frac{\mathrm{d}}{\mathrm{d}\theta}\left(\sin\theta \frac{\mathrm{d}g(\theta)}{\mathrm{d}\theta}\right), \tag{14}$$

$$\frac{1}{f(r)} \frac{\mathrm{d}}{\mathrm{d}r}\left(r^2 \frac{\mathrm{d}f(r)}{\mathrm{d}r}\right) + \Psi_2 r^2 = -\frac{1}{\sin\theta g(\theta)} \frac{\mathrm{d}}{\mathrm{d}\theta}\left(\sin\theta \frac{\mathrm{d}g(\theta)}{\mathrm{d}\theta}\right). \tag{15}$$

As a result, the variables are separated. We equate each side to a constant χ_1, χ_2 (which is independent of r and θ) and finally obtain

$$\frac{1}{\sin\theta} \frac{\mathrm{d}}{\mathrm{d}\theta}\left(\sin\theta \frac{\mathrm{d}g(\theta)}{\mathrm{d}\theta}\right) + \chi_1 g(\theta) = 0, \ \frac{1}{\sin\theta} \frac{\mathrm{d}}{\mathrm{d}\theta}\left(\sin\theta \frac{\mathrm{d}g(\theta)}{\mathrm{d}\theta}\right) + \chi_2 g(\theta) = 0, \tag{16}$$

$$\frac{1}{r^2} \frac{\mathrm{d}}{\mathrm{d}r}\left(r^2 \frac{\mathrm{d}f(r)}{\mathrm{d}r}\right) + \Psi_1 f(r) - \frac{\chi_1 f(r)}{r^2} = 0, \ \frac{1}{r^2} \frac{\mathrm{d}}{\mathrm{d}r}\left(r^2 \frac{\mathrm{d}f(r)}{\mathrm{d}r}\right) + \Psi_2 f(r) - \frac{\chi_2 f(r)}{r^2} = 0. \quad (17)(18)$$

Considering the possible χ values, Eq. (16) is customarily expressed in terms of the variable $x=\cos\theta$,

$$\left(1-x^2\right)\frac{\mathrm{d}^2 g_{\nu_1}\left(x\right)}{\mathrm{d}x^2}-2x\frac{\mathrm{d}g_{\nu_1}\left(x\right)}{\mathrm{d}x}+\nu_1\left(\nu_1+1\right)g_{\nu_1}\left(x\right)=0, \tag{19}$$

$$\left(1-x^2\right)\frac{\mathrm{d}^2 g_{\nu_2}\left(x\right)}{\mathrm{d}x^2}-2x\frac{\mathrm{d}g_{\nu_2}\left(x\right)}{\mathrm{d}x}+\nu_1\left(\nu_1+1\right)g_{\nu_2}\left(x\right)=0, \tag{20}$$

where the parameters χ_1 and χ_2 has been replaced by $\nu_1\left(\nu_1+1\right)$ and $\nu_2\left(\nu_2+1\right)$.The solution to the above equation is so-called Legendre functions which can be written through hypergeometric function

$$g_{\nu_1}\left(x\right)={}_2F_1\left(-\nu_1,\nu_1+1;1;\frac{1-x}{2}\right),\ g_{\nu_2}\left(x\right)={}_2F_1\left(-\nu_2,\nu_2+1;1;\frac{1-x}{2}\right). \tag{21}$$

Furthermore, Eqs (17) can be expanded into

$$r^2\frac{\mathrm{d}^2 f\left(r\right)}{\mathrm{d}r^2}+2r\frac{\mathrm{d}f\left(r\right)}{\mathrm{d}r}+\left[\Psi_1 r^2-\nu_1\left(\nu_1+1\right)\right]f\left(r\right)=0, \tag{22}$$

Similarly, Eq. (18) is expanded into

$$r^2\frac{\mathrm{d}^2 f\left(r\right)}{\mathrm{d}r^2}+2r\frac{\mathrm{d}f\left(r\right)}{\mathrm{d}r}+\left[\Psi_2 r^2-\nu_2\left(\nu_2+1\right)\right]f\left(r\right)=0. \tag{23}$$

Thus, the general solutions to the above two equations are

$$f_1\left(r\right)=A_1\mathrm{h}_{\nu_1}^{(1)}\left(\sqrt{\Psi_1}r\right)+B_1\mathrm{h}_{\nu_1}^{(2)}\left(\sqrt{\Psi_1}r\right),\ f_2\left(r\right)=A_2\mathrm{h}_{\nu_2}^{(1)}\left(\sqrt{\Psi_2}r\right)+B_2\mathrm{h}_{\nu_2}^{(2)}\left(\sqrt{\Psi_2}r\right), \qquad (24)(25)$$

where $\mathrm{h}_{\nu_1}^{(1)}$, $\mathrm{h}_{\nu_1}^{(2)}$, $\mathrm{h}_{\nu_2}^{(1)}$, and $\mathrm{h}_{\nu_2}^{(2)}$ are the spherical Hankel functions. In conclusion, the complete solution for the acoustic temperature in Eq. (8) becomes

$$T_1'\left(r,\theta;\frac{\omega}{c_0}\right)=\left[A_1\mathrm{h}_{\nu_1}^{(1)}\left(\sqrt{\Psi_1}r\right)+B_1\mathrm{h}_{\nu_1}^{(2)}\left(\sqrt{\Psi_1}r\right)\right]{}_2F_1\left(-\nu_1,\nu_1+1;1;\frac{1-\cos\theta}{2}\right), \tag{26}$$

$$T_2'\left(r,\theta;\frac{\omega}{c_0}\right)=\left[A_2\mathrm{h}_{\nu_2}^{(1)}\left(\sqrt{\Psi_2}r\right)+B_2\mathrm{h}_{\nu_2}^{(2)}\left(\sqrt{\Psi_2}r\right)\right]{}_2F_1\left(-\nu_2,\nu_2+1;1;\frac{1-\cos\theta}{2}\right). \tag{27}$$

It should be noticed that A_1, B_1, B_1 and B_2 are constant coefficients to be determined by the boundary conditions at the cross-sections $r=a$ and b of the truncated cone. Clearly, two different types of disturbance can propagate in the waveguide. Inserting the above two equations into Eq. (4) yields the expression of acoustic pressure

$$p_1'=\left[A_1\mathrm{h}_{\nu_1}^{(1)}\left(\sqrt{\Psi_1}r\right)+B_1\mathrm{h}_{\nu_1}^{(2)}\left(\sqrt{\Psi_1}r\right)\right]\left(\rho_0 c_p+\frac{\kappa_{\mathrm{th}}}{\mathrm{i}\omega}\Psi_1\right){}_2F_1\left(-\nu_1,\nu_1+1;1;\frac{1-\cos\theta}{2}\right), \tag{28}$$

$$p_2'=\left[A_1\mathrm{h}_{\nu_2}^{(1)}\left(\sqrt{\Psi_1}r\right)+B_1\mathrm{h}_{\nu_2}^{(2)}\left(\sqrt{\Psi_1}r\right)\right]\left(\rho_0 c_p+\frac{\kappa_{\mathrm{th}}}{\mathrm{i}\omega}\Psi_2\right){}_2F_1\left(-\nu_2,\nu_2+1;1;\frac{1-\cos\theta}{2}\right). \tag{29}$$

3. Simplified model of inviscid fluid

In the case of inviscid fluid, the thermoviscous dissipation is neglected in the wave propagation. As a result, acoustic wave is isentropic, which yields

$$\mathrm{i}\omega\rho'+\rho_0\nabla\cdot\mathbf{v}'=0,\mathrm{i}\omega\rho_0\mathbf{v}'=-\nabla p',\ p'=R_0 T\rho'. \tag{30}$$

Further deduction shows that

$$\nabla^2 p'+\frac{\omega^2}{R_0 T}p'=0, \tag{31}$$

which is consistent with the work of Willatzen [25] without flow. Similar deduction from section 2 can leads to the expression of

$$p' = \sum_{\nu} \left[A\mathrm{h}_{\nu}^{(1)} \left(\omega r / \sqrt{\gamma R_0 T} \right) + B\mathrm{h}_{\nu}^{(2)} \left(\omega r / \sqrt{\gamma R_0 T} \right) \right] {}_2F_1 \left(-\nu, \nu + 1; 1; \frac{1 - \cos\theta}{2} \right). \quad (32)$$

It should be noticed that under the intial $\theta = 0^{\mathrm{o}}$, the acoustic pressure is bounded. At the boundary condition $\theta = \theta_0$, the acoustic velocity vanishes, which leads to the

$$v'_{\theta}\big|_{\theta=\theta_0} = 0 \Rightarrow \left. \frac{\mathrm{d}g_{\nu}}{\mathrm{d}x} \right|_{x=\cos\theta_0} = 0, \quad (33)$$

where g_{ν} is defined by Eq. (21). Similarly, A and B are constant parameters to be determined by the boundary conditions at the cross-sections $r = a$ and $r = b$ of the truncated cone. A comprehensive deduction can be found in the work of Willatzen [25]. It should be noticed that the boundary condition in Eq. (33) is applicable to the thermovsicous case as shown in Eqs. (26) and (27), which means that $\nu = \nu_1 = \nu_2$.

4. Numerical study

In the section, numerical study is presented to analyse features of wave propagation. It should be noticed that the designation of propagation constants such as wave number and phase speed lose much of their intuitive meaning in a conical waveguide. Instead, the feature of wave propagation can be expressed in local wave number. By analogy with the cylindrical case, one can define the local wave number

$$k_{\nu}(r) = \mathrm{i} \frac{\partial f_{\nu} / \partial r}{f_{\nu}}. \quad (34)$$

As the boundary conditions at $r = a$ and $r = b$ are not specified, acoustic wave can propagate from a to b and vice versa. In the following study, one can denote that wave propagation from a to b is downstream and the other direction is upstream.

In the numerical study, the parameters are for perfect gas at $20\,^{\mathrm{o}}\mathrm{C}$, which are $\beta T_0 = 1$, $\rho_0 = 0.35\,\mathrm{kg/m^3}$, $\kappa_{\mathrm{th}} = 0.0674\,\mathrm{W}/(\mathrm{K}\cdot\mathrm{m})$, $\eta = 4.15\times10^{-5}\,\mathrm{kg}/(\mathrm{s}\cdot\mathrm{m})$, $\zeta = 0$, $\gamma = 1.4$, $R_0 = 287\,\mathrm{J}/(\mathrm{Kg}\cdot\mathrm{K})$, $c_p = 1184\,\mathrm{J}/(\mathrm{Kg}\cdot\mathrm{K})$, $T_0 = 293\mathrm{K}\left(20\,^{0}\mathrm{C}\right)$, $c_0 = \sqrt{\gamma T_0 R_0} = 343\,\mathrm{m/s}$. Assuming the opening angle θ_0 is 10^{o}, 20^{o} and 30^{o} respectively, the lowest four values for ν in Eq. (33) are listed as follows.

Table 1. Calculated ν values for a con with opening angles: $\theta_0 = 10, 20, 30$. The lowest four values are given for each opening angle θ_0

θ_0/mode index	1	2	3	4
10	0	21.5	39.7	57.8
20	0	10.5	19.6	38.4
30	0	6.8	18.9	25.0

The radii of the circular cross-section at the two ends are assumed to be 0.02 and 0.2m. Furthermore, the acoustic frequency to be investigated is $f = 10\mathrm{KHz}$. Figures 1-2 compare the difference of relative phase velocity ($1/K_{\mathrm{R}}$)and attenuation coefficient ($A = \left|8.686 k_0 K_{\mathrm{I}}\right|$) among three different wave modes as shown in Eqs. (26), (27) and (32) for the first two modes. Figure 3 concentrates on the relative phase velocity and attenuation coefficient of the second mode under different opening angles. From figures 1 and 2, it can be learned that the difference of the relative phase velocity and attenuation coefficient among the three different modes is relatively small when $\nu = 0$. However, the difference becomes explicit when $\nu = 21.5$.

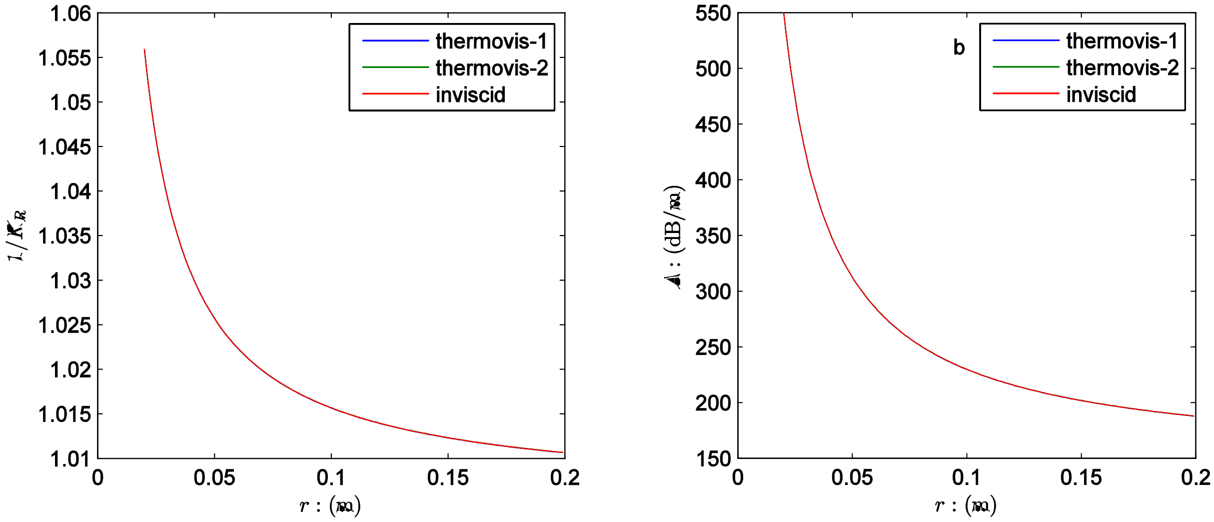

Figure 1. Comparison with inviscid and thermoviscous wave propagation in the r direction with the angles $\theta_0 = 10$ for the first mode. 'thermovis-1' represents the wave propagation in Eq. (26) and 'thermovis-2' represents the wave propagation in Eq. (27). 'inviscid' represents wave propagation in Eq. (32)

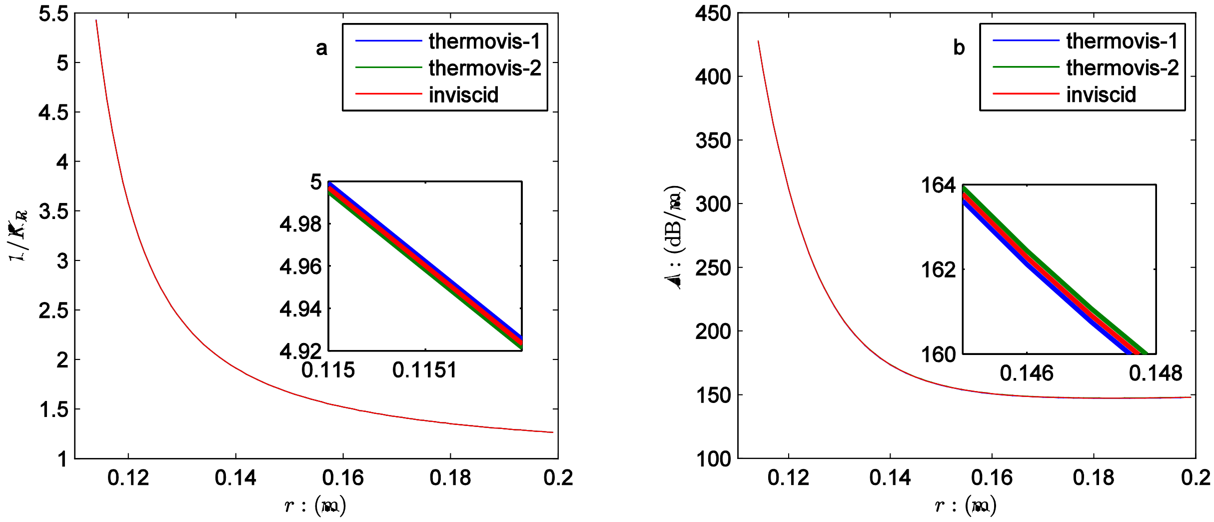

Figure 2. Comparison with inviscid and thermoviscous wave propagation in the r direction for the second mode. See Figure 1 for legend's description.

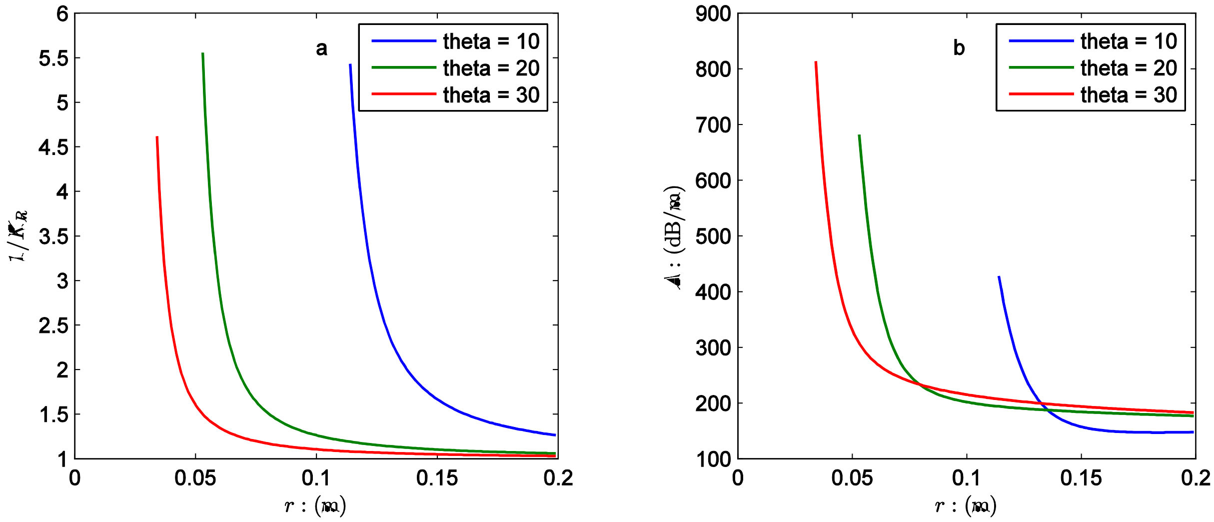

Figure 3. Comparison with inviscid and thermoviscous wave propagation in the r direction for different opening angles for the second mode with respect with ν.

From figure 3, it can be learned that the effect of opening angle on the features of wave propagation is significant. With the increase of opening angle, the existence of wave mode becomes easy.

5. Conclusion

Present paper concentrates on the thermovicous dissipation on wave propagation in a conical-confined pipeline. Comprehensive deduction of thermoviscous acoustic wave is formulated based on the conservations of mass, momentum and energy when the fluid is stationary. Numerical study is concentrated on the comparison of phase velocity and attenuation coefficient among different wave modes. Moreover, effect of opening angles of a conical pipeline on propagation features is analysed. The work described in this paper is funded by the National Natural Science Foundation of China(No. 11404405, 11504427, 61601489, and 51675525), the Major Program of National Natural Science Foundation of China (No. 61690210 and 61690213) and by the National Innovation Training Project of Undergraduate Student(No. 20169002001). The authors gratefully acknowledge the funding.

REFERENCES

1 Vilenski, G. G. and Rienstra, S. W. On hydrodynamic and acoustic modes in a ducted shear flow with wall lining, *Journal of Fluid Mechanics*, **583**, 45-70, (2007).

2 Brambley, E. J., Darau, M. and Rienstra, S. W. The critical layer in linear-shear boundary layers over acoustic linings, *Journal of Fluid Mechanics*, **710**, 545-568, (2012).

3 Zhang, C.-Y., Gao, J., Li, H., Song, L. and Lu, C. Propagation characteristics of surface acoustic waves in single-electron transport devices and the electrical measurement, *IEEE Transactions on Ultrasonics, Ferroelectrics, and Frequency Control*, **58** (7), 1452-1459, (2011).

4 Sankaranarayanan, S. K. R. S. and Bhethanabotla, V. R. Numerical analysis of wave generation and propagation in a focused surface acoustic wave device for potential microfluidics applications, *IEEE Transactions on Ultrasonics, Ferroelectrics, and Frequency Control*, **56** (3), 631-643, (2009).

5 Huttunen, T., Malinen, M., Kaipio, J. P., White, P. J. and Hynynen, K. A full-wave helmholtz model for continuous-wave ultrasound transmission, *IEEE Transactions on Ultrasonics, Ferroelectrics, and Frequency Control*, **52** (3), 397-409, (2005).

6 Brambley, E. J., Davis, A. M. J. and Peake, N. Eigenmodes of lined flow ducts with rigid splices, *Journal of Fluid Mechanics*, **690**, 399-425, (2012).

7 Khaletskiy, Y. D. Effectiveness of combined aircraft engine noise suppressors, *Acoustical Physics*, **58** (4), 556-562, (2012).

8 Oppeneer, M., Rienstra, S. W. and Sijtsma, P. Efficient mode matching based on closed-form integrals of Pridmore-Brown modes, *AIAA Journal*. 10.2514/1.J054167, (2015).

9 Rienstra, S. W., Darau, M. and Brambley, E. J. The trailing vorticity field behind a line source in two-dimensional incompressible linear shear flow, *Journal of Fluid Mechanics*, **720**, 618-636, (2013).

10 Peat, K. S. A first approximation to the effects of mean flow on sound propagation through cylindrical capillary tubes, *Journal of Sound and Vibration*, **175** (4), 475-489, (1994).

11 Peat, K. S. and Kirby, R. Acoustic wave motion along a narrow cylindrical duct in the presence of an axial mean flow and temperature gradient, *Journal of the Acoustical Society of America*, **107** (4), 1859-1867, (2000).

12 Chen, Y., Huang, Y. and Chen, X. Ultrasonic wave propagation in thermoviscous moving fluid confined by heating pipeline and flow measurement performance, *Journal of the Acoustical Society of America*, **134** (3), 1863-1874, (2013).

13 Chen, Y., Huang, Y. and Chen, X. Viscothermal longitudinal wave propagation in non-uniform shear liquid flow confined by constant temperature pipeline and implications for ultrasonic flow meter, *Acta Acustica United with Acustica*, **99** (6), 875-890, (2013).
14 Hosokawa, A. Ultrasonic pulse waves in cancellous bone analyzed by finite-difference time-domain methods, *Ultrasonics*, **44**, 227-231, (2006).
15 Chen, Y., Huang, Y. and Chen, X. Fourier-Bessel theory on flow acoustics in inviscid shear pipeline fluid flow, *Communications in Nonlinear Science and Numerical Simulation*, **18** (11), 3023-3035, (2013).
16 Chen, Y., Chen, X., Huang, Y., Bai, Y., Hu, D. and Fei, S. Study of thermoviscous dissipation on axisymmetric wave propagating in a shear pipeline flow confined by rigid wall. Part I. Theoretical formulation, *Acoustical Physics*, **62** (1), 27-37, (2016).
17 Chen, X., Chen, Y., Huang, Y., Bai, Y., Hu, D. and Fei, S. Study of thermoviscous dissipation on axisymmetric wave propagating in a shear pipeline flow confined by rigid wall. Part II. Numerical study, *Acoustical Physics*, **62** (2), 143-150, (2016).
18 Dokumaci, E. On the effect of viscosity and thermal conductivity on sound propagation in ducts: A re-visit to the classical theory with extensions for higher order modes and presence of mean flow, *Journal of Sound and Vibration*, **333**, 5583-5599, (2014).
19 Dokumaci, E. On transmission of sound in circular and rectangular narrow pipes with superimposed mean flow, *Journal of Sound and Vibration*, **210** (3), 375-389, (1998).
20 Davies, P. A. L. and Doak, P. E. Spherical wave propagation in a conical pipe with mean flow, *Journal of Sound and Vibration*, **137** (2), 343-346, (1990).
21 Davies, P. A. L. and Doak, P. E. Wave transfer to and from conical diffusers with mean flow, *Journal of Sound and Vibration*, **138** (2), 345-350, (1990).
22 Easwaran, V. and Munjal, M. L. Plane wave analysis of conical and exponential pipes with incompressible mean flow, *Journal of Sound and Vibration*, **152** (1), 73-93, (1992).
23 Munjal, M. L. *Acoustics of ducts and mufflers*, John Wiley & Sons Ltd, Unidted Kingdom, (2014).
24 Mimani, A. Acoustical behaviour of conical muffler with single-inlet and single-outlet: a 3-D semi-analytical approach, *Acousics* (2015).
25 Willatzen, M. The influence of a liquid flow on sound fields confined by conical walls, *Journal of Sound and Vibration*, **248** (5), 847-863, (2001).
26 Astley, R. J. and Eversman, W. A finite element method for transmission in non-uniform ducts without flow: comparison with the method of weighted residuals, *Journal of Sound and Vibration*, **57** (3), 367-388, (1978).
27 Eversman, W. and Astley, R. J. Acoustic transmission in non-uniform ducts with mean flow. Part I: the method of weighted residuals, *Journal of Sound and Vibration*, **74** (1), 89-101, (1981).